

Article

Ru-gC₃N₄ Catalyzed Hydrodebenzylation of Benzyl Protected Alcohol and Acid Groups Using Sodium Hypophosphite as a Hydrogen Source

Sourav Chakraborty * , Ashish Bahuguna * and Yoel Sasson

Casali Center of Applied Chemistry, Institute of Chemistry, The Hebrew University of Jerusalem, Jerusalem 9190401, Israel; ysasson@huji.ac.il

* Correspondence: sourav.chakraborty@mail.huji.ac.il (S.C.); ashish.bahuguna@mail.huji.ac.il (A.B.); Tel.: +972-2-658-5111 (S.C. & A.B.)

Abstract: A straightforward process for hydrodebenzylation of benzyl protected acid and alcohol derivatives to the corresponding acids and alcohols using sodium hypophosphite in the presence of Ru-GCN catalyst is reported. The developed Ru-GCN catalyst is cost effective compared to other noble metal-based catalysts and has been explored to exhibit excellent activity for catalytic hydrodebenzylation reactions under moderate reaction conditions. The non-corrosive sodium hypophosphite has been found as a better hydrogen donor compared to alkali metal formats in presence of Ru-GCN catalyst. The stated catalyst was characterized using several spectrometric and material characterization methods such as PXRD, IR, SEM, TEM, XPS, and TGA. The Ru-GCN catalyst corroborated good reusability and stability for multiple cycles. The catalyst preparation is facile and the developed process is simple and safe as it avoids use of high hydrogen pressure. The developed protocol can also be replicated on industrial scale on account of excellent recyclability and retained activity after multiple cycles and makes the process sustainable. Gram scale reaction was performed to verify the industrial potential of reported catalyst.

Keywords: heterogeneous catalyst; hydrogen transfer reaction; graphitic carbon nitride



Citation: Chakraborty, S.; Bahuguna, A.; Sasson, Y. Ru-gC₃N₄ Catalyzed Hydrodebenzylation of Benzyl Protected Alcohol and Acid Groups Using Sodium Hypophosphite as a Hydrogen Source. *Catalysts* **2021**, *11*, 1227. <https://doi.org/10.3390/catal11101227>

Academic Editor: Gilles Berhault

Received: 20 September 2021

Accepted: 8 October 2021

Published: 12 October 2021

Publisher's Note: MDPI stays neutral with regard to jurisdictional claims in published maps and institutional affiliations.



Copyright: © 2021 by the authors. Licensee MDPI, Basel, Switzerland. This article is an open access article distributed under the terms and conditions of the Creative Commons Attribution (CC BY) license (<https://creativecommons.org/licenses/by/4.0/>).

1. Introduction

Protection and de-protection of alcohol and acid groups is an important methodology in the field of fine chemicals and pharmaceutical industries. Researchers prefer this pathway to control side reactions during chemical transformations in these fields [1,2]. The most conventional used protection technique is the preparation of benzyl ether and ester during various drug syntheses [3,4]. It is straightforward method to prepare benzyl protecting group and has good stability during various chemical transformation reactions [5]. Therefore, this methodology has developed into a necessary tool to design a multistep route of organic synthesis in the fine chemicals and pharmaceutical industries as well as in basic or applied research [5–7]. Hence, it is essential to acquire a smooth and economical hydrodebenzylation protocol. Transition metal catalyzed hydrodebenzylation would thus be one of the best courses for future research and development in the above chemical industries. Catalytic hydrodebenzylation practice is the most useful method in this prospective and is a cost effective way being eco-friendly and sustainable process [8]. In literature, there are numerous catalytic procedures reported for hydrodebenzylation reaction comprising of both homogeneous and heterogeneous systems. Although many homogeneous catalysts have good activity and broad applicability, heterogeneous catalyst offers numerous advantages due to sustainability and industrial applicability. The leading benefits of heterogeneous catalyst are recyclability of the catalyst, easy separation from the reaction mixture, tolerance of critical reaction conditions, etc. According to the green chemistry point of view, the use of heterogeneous catalysts renders the chemical process

sustainable and environmentally friendly. Hence, the heterogeneous catalysts have been effectively used in various types of chemical transformation reaction including hydrodebenzylation. An improvement of these areas helps us to perform a chemical transformation reaction more efficiently, particularly in the usage of low-cost and more active catalysts.

There are several catalytic systems reported for the hydrodebenzylation protocol and some of the latter use transition metal catalysts. The major catalytic methods used for this reaction through the past few decades are Pd [2,9–14], Pt [15], Rh [16], Ru [17–19], Raney Ni [20,21], Ni [22–24], Cu [25], Co [26], and on occasion bimetallic [13,14,17,27–29]. The majority of these metal catalysts were applied as homogeneous catalysts and several as heterogeneous. In most cases, Pd has been used as a catalyst of choice for hydrodebenzylation reaction. Despite the numerous applications reported in the literature, hydrodebenzylation using Pd has several drawbacks such as high cost, catalyst deactivation due to metal oxidation, and change in particle size distribution of metal on the support. Another serious issue with Pd metal is its pyrophoric nature. The latter depends on the on metal loading and causes serious handling issues even in lab scale reactions. The most commonly used hydrogen donors for the hydrodebenzylation or transfer hydrogenation reactions are sodium borohydride [24], lithium aluminum hydride [26], 2-propanol [11,29], formic acid [2], alkali metal formates [30], sodium hypophosphite [10], supercritical ethanol [31], and molecular hydrogen. Most of these hydrogen sources have been used with the Pd metal catalyst. Alkali hypophosphite salts behave as an effective hydrogen donor in presence of a metal catalyst [32,33]. It decomposes to molecular hydrogen and sodium hydrogen phosphite in presence of catalyst and water. Hence, we aspired to develop a cost effective hydrodebenzylation system catalyzed by metal catalyst using transfer hydrogen methodologies using sodium hypophosphite as a hydrogen donor. This approach is safe and cost effective compared to molecular hydrogen in high pressure cylinder. In contrast to previous studies we have opted to focus on ruthenium as the catalytic metal. Ru is reasonably priced in comparison with Pd, Pt, and Rh. In this study, we report a ruthenium metal supported on graphitic carbon nitride as a novel catalyst for the hydrodebenzylation reaction of benzylic protected alcohol and acid groups using NaH_2PO_2 as a hydrogen source. The process is depicted in Figure 1. The latter is evidently a smooth, safe and cost effective protocol for hydrodebenzylation reactions.

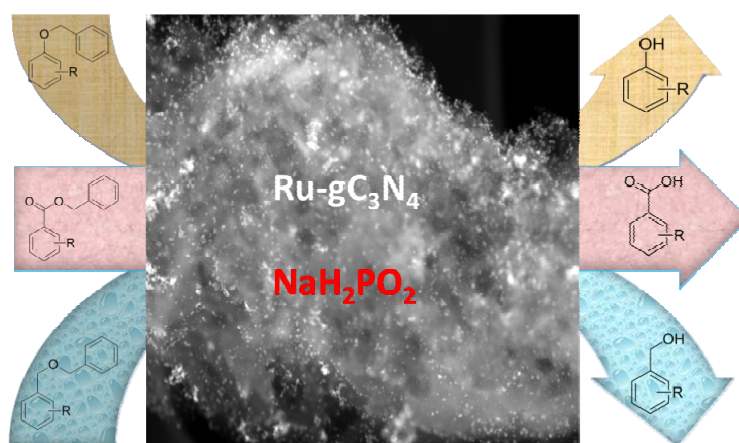


Figure 1. Schematic representation of Ru-GCN catalyzed hydrodebenzylation reaction.

2. Results

The fabricated materials, graphitic carbon nitride (GCN) and $\text{Ru-gC}_3\text{N}_4$ (Ru-GCN), were characterized using several microscopic and spectral methods. The powder X-ray diffraction (PXRD) pattern of GCN and Ru-GCN is shown in Figure 2. PXRD analysis of the samples provides detail regarding the phase purity of the prepared material. The PXRD graph of GCN shows two characteristic peaks of GCN at 12.9° and 27.4° . The diffraction peak at 12.9° corresponds to (100) diffraction plane. It has mild diffraction because of inter-planer separation. The intensity of this peak is also low as compared to the peak

27.4° which correspond to the diffraction plane of (002). The intensity of this peak is high because of the inter-planer-d spacing and π - π stacking of the conjugated aromatic system. Similarly, in case of Ru-GCN, it shows the additional peaks at 43.6°, 57.6°, 69.1°, and 83.9° for Ru. These peaks are corresponds to (101), (102), (110), and (103) diffraction planes of Ru nanoparticles, respectively.

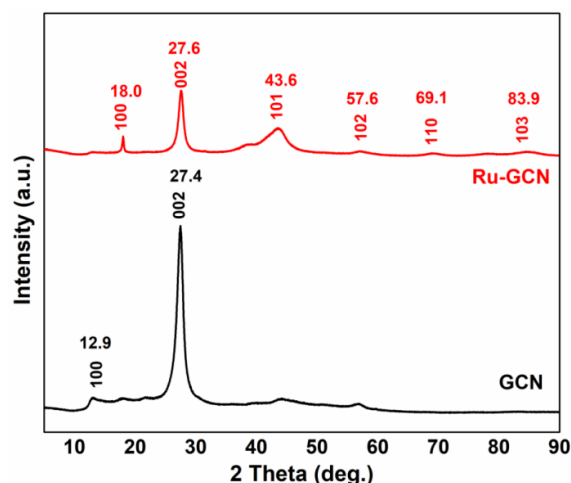


Figure 2. Powder X-ray diffraction (PXRD) patterns of GCN and Ru-GCN.

GCN and Ru-GCN have been analyzed using Fourier-transform infrared spectroscopy (FTIR). It shows the presence of chemical functionality in the material. The FTIR spectra of GCN and Ru-GCN are shown in the Figure 3. The broad absorption band in the range 3000 to 3400 cm^{-1} was observed because of N-H stretching vibrations. The peaks at 1390 cm^{-1} indicates the C-N stretching vibration, while 1620 cm^{-1} corresponds to C=N stretching vibration of the aromatic triazine ring system. The absorption band 798 cm^{-1} corresponds to the triazine ring system in the GCN material. In case of Ru-GCN material, it is found that the broadness and intensity of the peak which indicates N-H stretching vibration are decreased strongly. Hence, it can be contemplated that it is due to the Ru metal interaction with GCN material. Moreover, the intensity of the peak 1530 cm^{-1} also decreases to a great extent after formation of Ru-GCN nanocomposite from GCN.

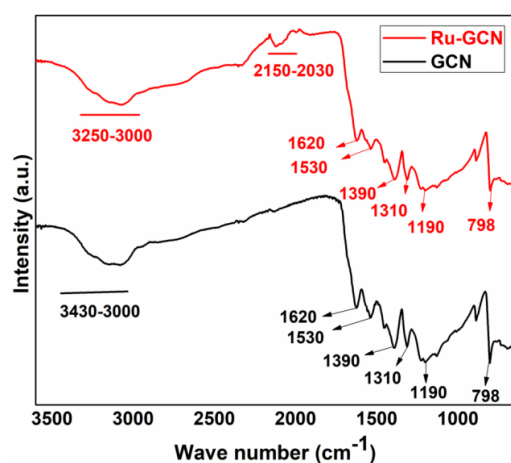


Figure 3. Fourier Transform Infra-red (FTIR) spectra of GCN and Ru-GCN.

The elemental composition and morphology of the fabricated Ru-GCN catalyst was performed by scanning transmission electron microscopy (STEM) and transmission electron microscopy (TEM). From Figure 4, it is observable that the Ru particles are distributed everywhere on the surface of graphitic carbon nitride nanosheets. The average size of

the Ru nanoparticles on the GCN surface has been found to be around 1–2 nm and the particles are distributed effectively throughout the support surface (Figure 4c). The particle distribution curve of the Ru nanoparticles (Figure 4d) shows that the maximum populated particle size is in the range of 1.5 to 1.6 nm. Energy dispersive spectroscopy (EDS) analysis of the Ru-GCN material further proves the presence of the component elements such as C, N, O and Ru in the prepared material (Figure S1 and Table S1). The elemental mapping of Ru-GCN catalyst shows presence and the distribution of elements such as C, N, O, and Ru in the Ru-GCN material (Figure S2). The elemental composition analysis of the Ru-GCN material was performed by SEM-EDS and which further confirmed 3.85 wt% Ru metal present over the Ru-GCN material (Figure S3 and Table S2).

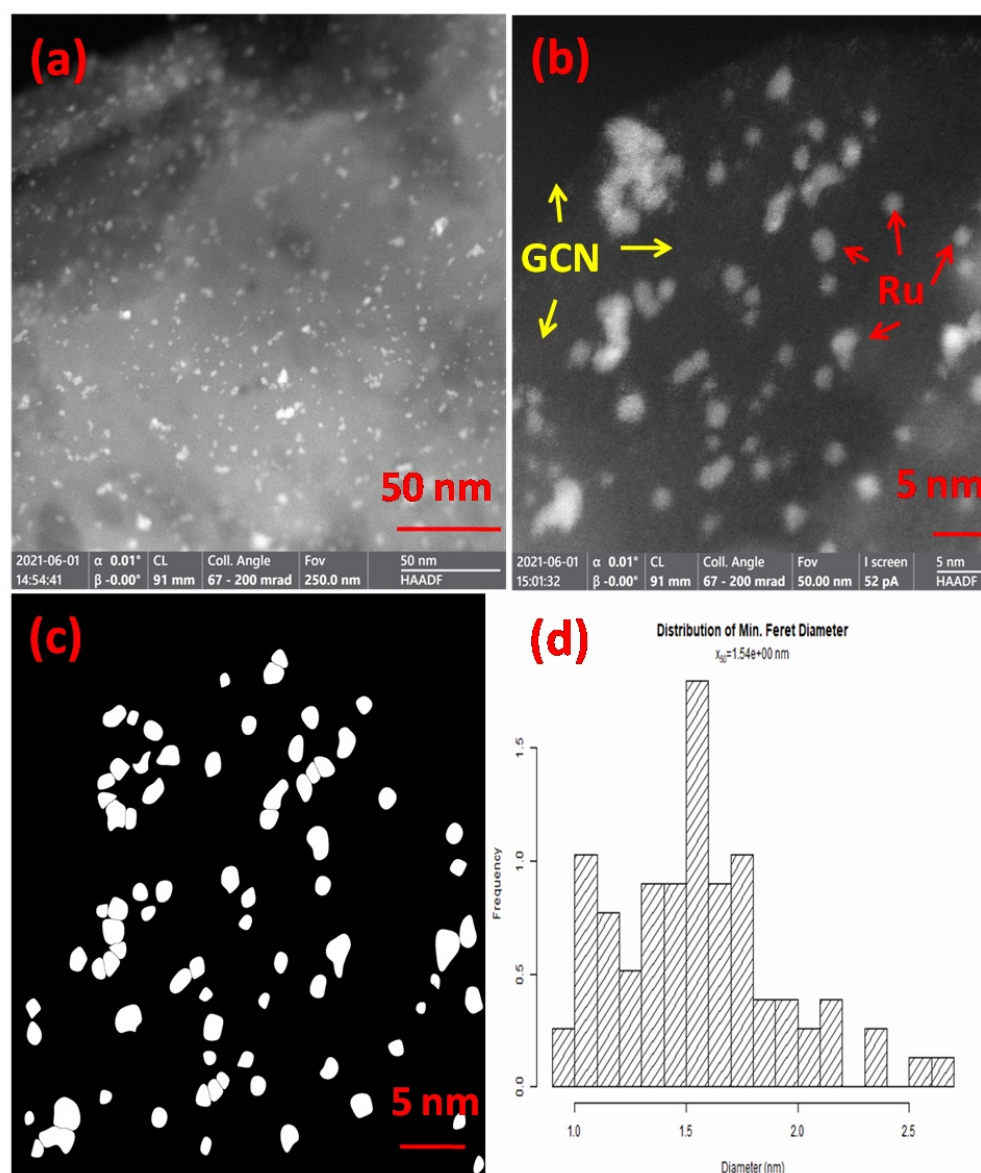


Figure 4. Scanning transmission electron microscopy (STEM) images of Ru-GCN (a–d) particle size distribution curve of Ru in Ru-GCN.

The chemical state and elemental composition of the Ru-GCN was studied using X-ray photoelectron spectroscopy (XPS) as shown in Figure 5. The presence of carbon, nitrogen, oxygen, and ruthenium elements in the prepared sample are shown in the survey spectrum of the Ru-GCN material (Figure 5d). The deconvoluted spectrum of C 1s, N 1s, O 1s, and Ru 3d of Ru-GCN catalyst are shown in Figure 5a–c. The deconvoluted spectrum of C 1s shows

peaks at 285.0, 286.3, and 288.6 eV, respectively, for the various varieties of carbon atoms present in the Ru-GCN material. The deconvoluted N1s spectrum of Ru-GCN shows peaks at 399.1, and 400.4 eV for the pyridinic, and pyrrolic and atoms present in the Ru-GCN material, respectively. The deconvoluted spectrum of Ru 3d shows peaks at 280.3, 282.2, 284.5, and 286.1, respectively. The peaks at 280.3 eV and 284.5 eV represent the Ru 3d_{5/2} and Ru 3d_{3/2} electronic state of Ru metal in the zero oxidation state, respectively. Similarly, the peaks at 282.2 eV and 286.1 eV represents the Ru 3d_{5/2} and Ru 3d_{3/2} electronic state of the Ru metal in Ru⁴⁺ oxidation state, respectively. The deconvoluted spectrum of O1s shows peaks at 529.6 and 532.1 eV and represents the presence of two forms of oxygen atoms in the material. The peak at 529.6 eV represents the surface adsorbed oxygen atom in the material while the peak at 532.1 eV can be attributed to the oxygen atom present in small amount of RuO₂ in the material. The elemental composition of Ru-GCN has determined by XPS and the results are presented in the Table S3.

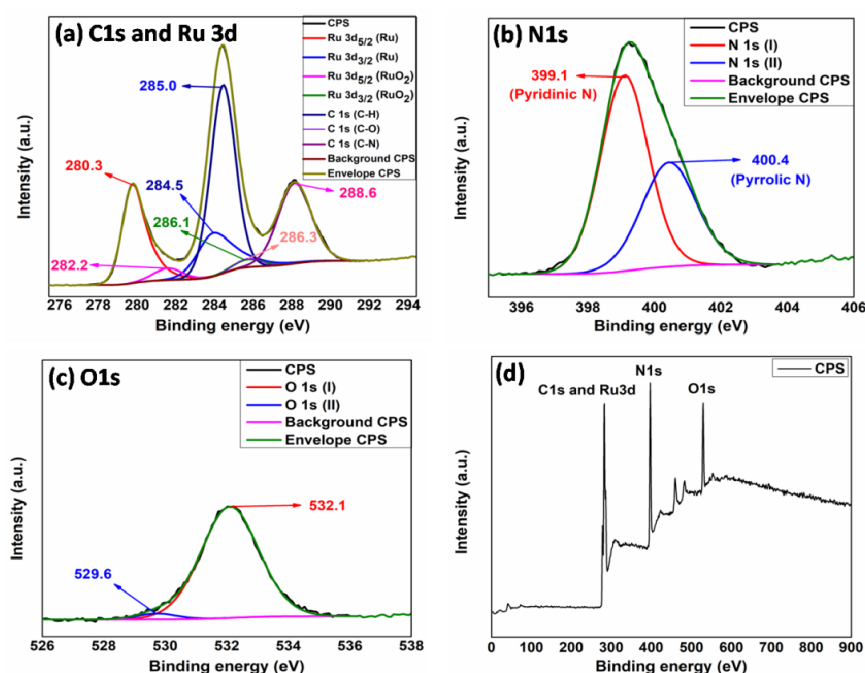


Figure 5. Deconvoluted X-ray photoelectron spectroscopy (XPS) spectrum of C1s and Ru 3d (a), N1s (b), O1s (c) and survey spectrum of elements (d) in Ru-GCN material.

The thermal stability of GCN and Ru-GCN was conducted by the thermo gravimetric analysis (TGA). The Figure 6 depicts the TGA analysis of GCN and Ru-GCN. It is observed that 5% weight loss up to 180 °C from both GCN and Ru-GCN corresponds to water or moisture evaporation from samples. After that GCN stays stable from 185 up to 500 °C and zero weight loss observed from the GCN sample. After 500 °C, GCN start losing weight sharply and it losses 94.6% weight up to 740 °C. Likewise, Ru-GCN nanocomposit shown stability up to 220 °C. After 220 °C, it started decompose continuously up to 600 °C. In case of Ru-GCN, 90.7% weight loss observed up to 600 °C. From the difference of the weight loss observed of GCN and Ru-GCN, we can calculate the metal percentage (3.95%) in the Ru-GCN catalyst. Moreover, from the thermogravimetric analysis graph of GCN and Ru-GCN, it can be summarized that the stability of GCN has highly declined from 500 °C to 220 °C by the formation of Ru-GCN nanocomposite.

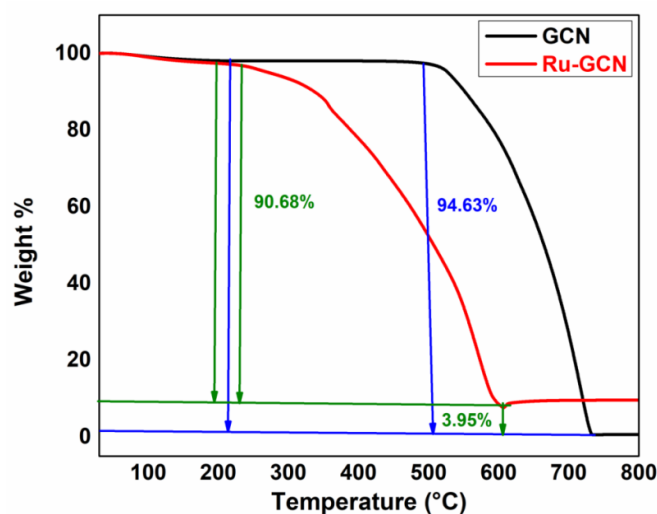
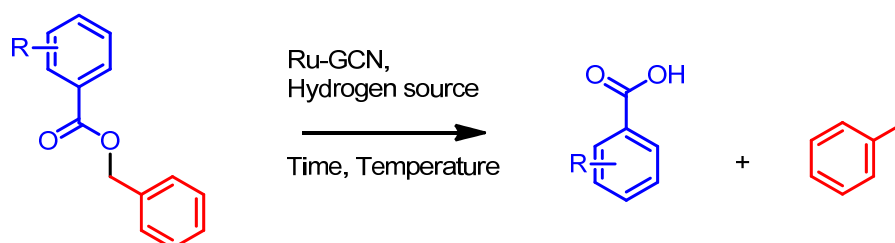


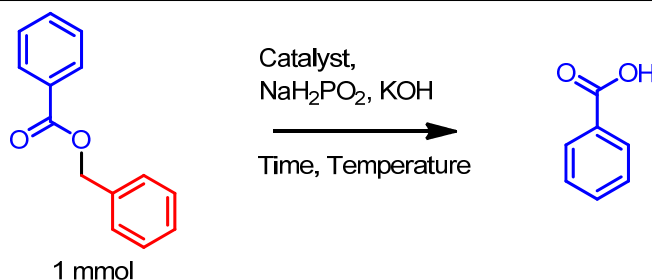
Figure 6. Thermogravimetric analysis (TGA) of GCN and Ru-GCN material.

Catalytic Activity Studies

The activity of the Ru-GCN catalyst was investigated for the hydrodebenzylation reaction of benzyl protected alcohol and acid groups. The Ru-GCN catalyst has very good potential to release hydrogen from Sodium hypophosphite solution. Hence, Sodium hypophosphite was chosen as a hydrogen source for hydrodebenzylation reaction. The Ru-GCN catalyzed hydrodebenzylation of acid or alcohol groups is shown in the Scheme 1. The activity of Ru-GCN catalyst for hydrodebenzylation reaction was investigated with a substrate, namely benzyl benzoate using NaH_2PO_2 as a hydrogen source. Various reaction parameters were examined and details are presented in the Table 1. It is very clear from Table 1 that the reaction does not precede at low temperature (Entry No. 1–3). Even at 50°C , the reaction shows no conversion of starting material. Though, we performed the reaction with double quantity catalyst and reagents at room temperature, again after 24 h no conversion was observed (Entry No. 2). The best result was observed at 110°C and where up to 95% isolated yield was measured (Entry No. 5). During catalyst optimization, we found that 42 mg catalyst provides us better results for 1 mmol of the substrate (Entry No. 5–7). The minimum requirement of hydrogen source was observed 2.0 eq. with respect to substrate (Entry No. 5, 8, 9). It was also noted that addition of KOH had a positive impact on activity and complete conversion of starting material was realized (Entry No. 9–11). In absence of KOH, we observed only 40% yield (Entry No. 11). We confirmed that presence of water is a mandatory requirement for the completion of reaction. This is due to non-solubility of sodium hypophosphite in ethanol (Entry No. 14). Therefore, EtOH/ H_2O combination was corroborated as a solvent for hydrodebenzylation reaction in presence of sodium hypophosphite as a hydrogen source. In addition other solvent-water mixture combinations were also optimized (Entry No. 5 and 14–16).



Scheme 1. Representative reaction of Ru-GCN catalyzed hydrodebenzylation reaction.

Table 1. The optimization of Ru-GCN catalyzed hydrodebenzylation reaction.

Entry No.	Ru-GCN (mg)	NaH ₂ PO ₂ (eq.)	KOH Additive (eq.)	Solvent	Temp. (°C)	Time (h)	Yield (%)
1	42	2.0	2.0	1:1 EtOH/H ₂ O	RT	24	0
2	84	3.0	3.0	1:1 EtOH/H ₂ O	RT	24	0
3	42	2.0	2.0	1:1 EtOH/H ₂ O	50	24	0
4	42	2.0	2.0	1:1 EtOH/H ₂ O	80	24	40
5	42	2.0	2.0	1:1 EtOH/H ₂ O	110	8	95
6	21	2.0	2.0	1:1 EtOH/H ₂ O	110	8	70
7	00	2.0	2.0	1:1 EtOH/H ₂ O	110	24	0
8	42	1.0	2.0	1:1 EtOH/H ₂ O	110	8	60
9	42	3.0	2.0	1:1 EtOH/H ₂ O	110	8	95
10	42	2.0	1.0	1:1 EtOH/H ₂ O	110	8	65
11	42	2.0	00	1:1 EtOH/H ₂ O	110	8	40
12	42	2.0	2.0	1:1 EtOH/H ₂ O	110	6	82
13	42	2.0	2.0	1:1 EtOH/H ₂ O	110	4	65
14	42	2.0	2.0	EtOH	110	24	0
15	42	2.0	2.0	1:1 Dioxane/H ₂ O	110	8	20
16	42	2.0	0.0	1:1 AcOH/H ₂ O	110	8	0

Following the optimization of hydrodebenzylation reaction process for benzyl benzoate in presence of Ru-GCN catalyst and sodium hypophosphite as a hydrogen donor, we validated our protocol with several categories of substrates. Several examples of benzyl protected acid and alcohol group carrying different functionalities were hydrodebenzylated in presence of Ru-GCN catalyst. The experimented results are depicted in the Table 2.

Here, the potential of Ru-GCN catalyst was compared with the previously reported catalyst for the hydrodebenzylation reaction. The catalytic debenzylization reaction conditions and yield from the literature are presented in the Table 3. Most of the hydrodebenzylation reactions reported in literature were catalyzed by Pd or other homogeneous catalyst. Therefore, Ru-GCN catalyst due to cost effectiveness compared to Pd will be an effective catalyst for hydrodebenzylation reactions. Moreover, Ru-GCN catalyst is heterogeneous in nature and can be used for multiple cycles.

Finally a gram scale hydrodebenzylation reaction of benzyl benzoate (Scheme 2) was performed to check the industrial potential of our proposed Ru-GCN catalyst. The yield obtained for this substrate was 92%. The isolation of Ru-GCN catalyst was performed by centrifugation method. After completion of the reaction, the reaction mixture was centrifuged at 7000 rpm at room temperature. The isolated catalyst washed with distilled water (3 × 50 mL) followed by washing with ethanol (50 mL). The catalyst was dried in a hot oven at 80 °C for 16 h. The recycled catalyst was further used for multiple cycles. The results of recyclability study are presented in the Figure 7. It was verified that the recycled catalyst showed good activity after many cycles. The stability of the recycled Ru-GCN catalyst was checked by TGA data (Figure S6) and PXRD patterns (Figure S7) and found that there is no significant change in recovered Ru-GCN catalyst after multiple cycles with respect to the fresh Ru-GCN catalyst. Further stability of Ru-GCN catalyst was confirmed

by the TEM (Figure S4 and Table S4), SEM (Figure S5 and Table S5), and XPS (Table S6) analysis. Therefore, it is clear that our developed Ru-GCN catalyst has good activity as well as stability after multiple cycles.

Table 2. Substrate scope for the Ru-GCN catalyzed hydrodebenzylation reaction.

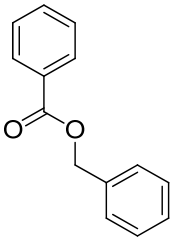
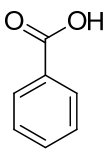
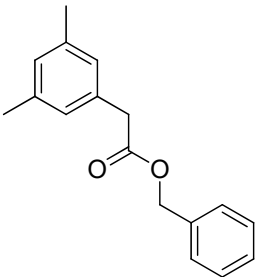
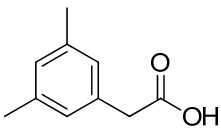
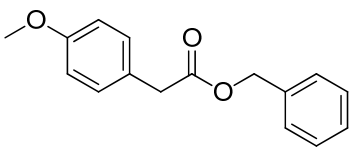
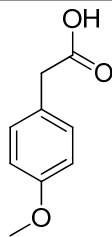
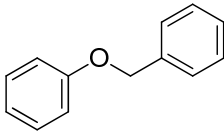
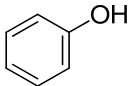
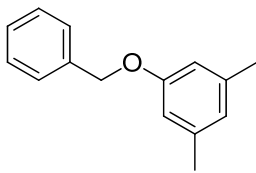
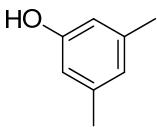
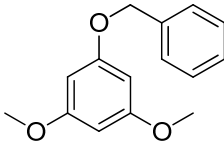
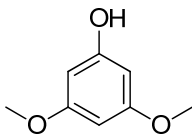
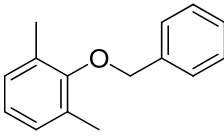
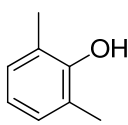
Sl. No	Substrate	Product	Isolated Yield (%)
1			95
2			93
3			93
4			90
5			86
6			88
7			85

Table 2. Cont.

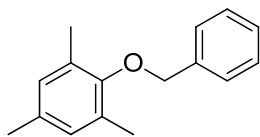
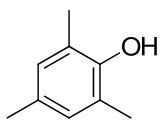
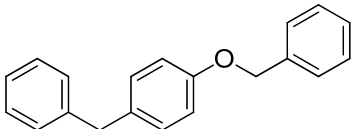
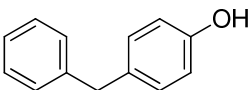
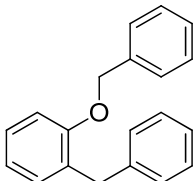
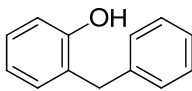
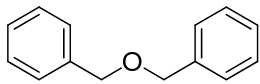
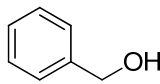
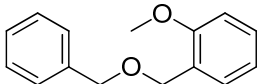
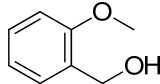
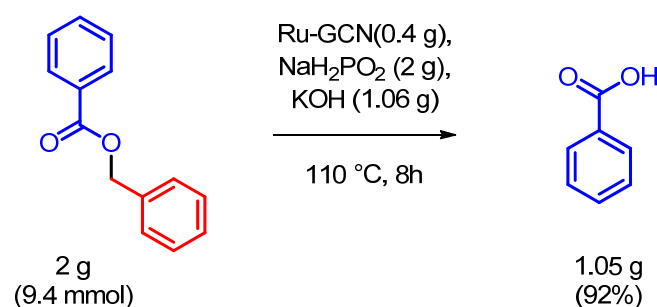
Sl. No	Substrate	Product	Isolated Yield (%)
8			85
9			88
10			83
11			92
12			89

Table 3. Comparison of catalytic activity of Ru-GCN Nanocomposite with other reported catalysts for the Hydrodebenzylation reaction.

Entry. No.	Catalyst	H ₂ Sources	Additive/Base	Nature of Catalyst	Temp. (°C)	Time (h)	Yield (%)	Ref.
1	Pd(OAc) ₂	Hydrogen (1 atm)	N/A	Het.	25 °C	14	99	[2]
2	Pd/C	Hydrogen (50 pSi)	N,O-bis(trimethylsilyl)acetamide(BSA) and Dabco	Het.	RT	8	88	[9]
3	Pd/AC	Sodium hypophosphite monohydrate	Tween 20 as a surfactant	Het.	50 °C	1	94	[10]
4	Pd/C	Sodium borohydride	N/A	Het.	80 °C	1	100	[24]
5	Pd/Co	2-isopropanol	N/A	Het.	240 °C	3	100	[11]
6	Pd/C	Ammonium formate	N/A	Het.	60 °C	1/2	100	[2]
7	Pd/C	Formic acid	KOH	Het.	70 °C	1	100	[2]
8	Ni/CB	Sodium borohydride	N/A	Het.	80 °C	2	90	[24]
9	Ru/AC	Molecular Hydrogen (25 bar)	N/A	Het.	150 °C	2	100	[19]
10	Ru/AC	Supercritical ethanol	N/A	Het.	270 °C	4	60	[31]
11	Ru-W/AC	Molecular Hydrogen (0.7 MPa)	N/A	Het.	260 °C	10	93	[17]
12	Indium triflate, Ru/Al ₂ O ₃	Molecular Hydrogen (580 pSi)	N/A	Het.	250 °C	2	80	[18]
13	Ru-gC ₃ N ₄	Sodium hypophosphite	KOH	Het.	110 °C	8	Upto 95	This work



Scheme 2. Gram scale reaction of Ru-GCN catalyzed hydrodebenzylation of benzyl benzoate (Appendix A).

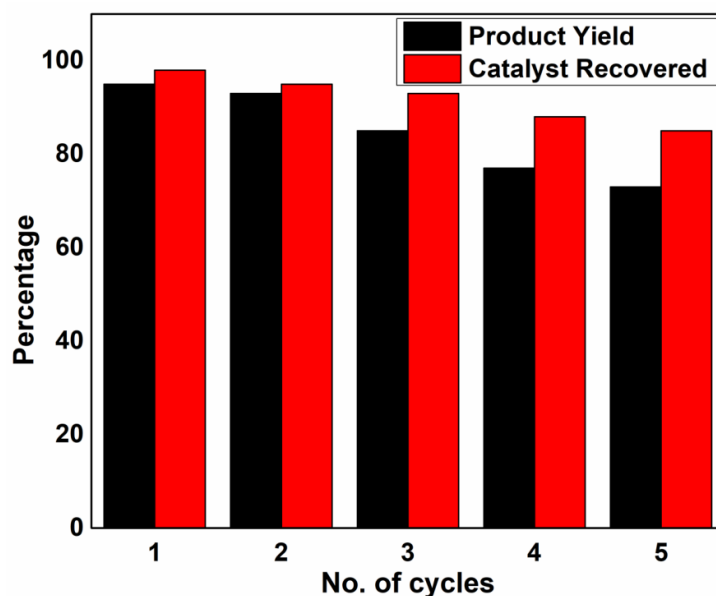


Figure 7. Recyclability test of Ru-GCN catalyst.

3. Material and Methods

3.1. Fabrication of Graphitic Carbon Nitride (GCN)

GCN was fabricated using a slightly modified well-known literature procedure [34] via thermal condensation of dicyandiamide followed by polymerization. In brief, dicyandiamide (10 gm) was placed in a medium size alumina crucible and heated to 550 °C for 3 h in a furnace at atmospheric air pressure with a ramp rate of 10 °C per minute. Afterwards, the obtained material light yellow in color was milled and further recalcined at a temperature of 550 °C for an additional 3 h. A total of 6.4 g of light yellow graphitic carbon nitride nanosheets was obtained and it was used without further treatment.

3.2. Synthesis of Ru-gC₃N₄ (Ru-GCN)

A total of 500 mg of graphitic carbon nitride was taken in a 100 mL flask. Then, 50 mL of demineralised water was added to the round bottom flask and the reaction mixture solution was stirred for 4 h at 25 to 30 °C. Then, 46 mg of RuCl₃.XH₂O dissolved in 20 mL of distilled water was added to the reaction mixture and stirred for another 2 h at 25 to 30 °C. Then, 42 mg of sodium borohydride was slowly added to the reaction mixture maintained at 25 to 30 °C for 15 min. Next, the reaction mixture was further allowed for stirring at 25 to 30 °C for an additional 24 h. Consequently, the produced catalyst was isolated by centrifugation technique and washed multiple times with water and ethanol to remove impurities/salts. The black color solid (Ru-GCN) was dried in a hot oven at 80 °C for 16 h. After drying, 485 g of Ru-GCN catalyst was obtained.

4. Conclusions

Ru-GCN catalyzed hydrodebenzylation by transfer hydrogen methodology was reported in this paper. Here, the sodium hypophosphite behaves as a non-corrosive hydrogen source for the transfer hydrogen methodology. Ru-GCN has been found as a cost effective catalyst for this reaction. Excellent recyclability and reusability for successive reaction cycles and the stability of the developed Ru-GCN confirms the sustainable and eco-friendly nature of the process. This protocol is safe as it avoids highly pyrophoric palladium metal and high hydrogen pressure cylinder. Green solvents such as water and ethanol are used for this process. The above presented results demonstrate a good and versatile process under moderate reaction condition to remove benzyl group from benzyl protected acid and alcohol compounds.

Supplementary Materials: The following are available online at <https://www.mdpi.com/article/10.3390/catal11101227/s1>, Figure S1: TEM image (a) and EDAX (b) of Ru-GCN, Figure S2: Elemental mapping of Ru-GCN material; (b) carbon, (c) nitrogen, (d) oxygen, and (e) ruthenium, Figure S3: SEM image (a) elemental quantification (b) of Ru-GCN material, Figure S4: TEM image (a) and EDAX (b) of recycled Ru-GCN catalyst, Figure S5: SEM image (a) elemental quantification (b) of recycled Ru-GCN catalyst, Figure S6: Comparison of TGA of fresh and recycled Ru-GCN catalyst, Figure S7: Comparison of XRD of fresh and recycled Ru-GCN catalyst, Table S1: Elemental composition of Ru-GCN material, Table S2: Elemental composition of Ru-GCN material, Table S3: XPS Elemental composition/Quantification of Ru-GCN, Table S4: Elemental composition of recycled Ru-GCN catalyst, Table S5: Elemental composition of recycled Ru-GCN catalyst, Table S6: XPS Elemental composition/Quantification of recycled Ru-GCN catalyst.

Author Contributions: Conceptualization, S.C. and A.B.; methodology, S.C. and A.B.; validation, S.C.; formal analysis, S.C.; investigation, S.C.; data curation, S.C.; Writing—original draft, S.C.; writing—review & editing, A.B. and Y.S.; visualization, S.C.; supervision, Y.S.; project administration, A.B. and Y.S.; funding acquisition, not applicable. All authors have read and agreed to the published version of the manuscript.

Funding: This research received no external funding.

Data Availability Statement: Data is contained within the article or Supplementary Materials.

Acknowledgments: Authors acknowledge the Casali Center of Applied Chemistry and Nano Center of The Hebrew University for the instrumentation facilities.

Conflicts of Interest: The authors declare no conflict of interest.

Appendix A

Experimental Section

Hydrodebenzylation of benzyl benzoate: In a glass pressure tube, 212 mg (1 mmol) of benzyl benzoate, 42 mg (0.017 mmol) of the Ru-GCN catalyst, 112 mg (2 mmol) of KOH, and 212 mg (2 mmol) of NaH_2PO_2 were charged and 4 mL of the solvent (1:1 mixture of EtOH + H_2O) was added. Then, the reaction was heated to 110 °C on an oil bath. Then, the reaction mixture was maintained at 110 °C for 8 h to get complete conversion from starting material to product. After completion of the reaction, the catalyst was separated by centrifugation and washed with EtOH. Then, the EtOH solvent was completely removed at rota vapour. The pH of the reaction mixture was adjusted to neutralize with dilute acetic acid. The desired product was isolated by extraction with ethyl acetate. Then, the ethyl acetate layer was evaporated on rotary evaporator to get the crude product. The obtained crude product was purified by silica gel column with the mixture of ethyl acetate and hexane as diluents to get the pure product (116 mg, Yield = 95%).

Gram Scale Reaction of Hydrodebenzylation of benzyl benzoate: In an autoclave, 2.0 g (9.4 mmol) of benzyl benzoate, 400 mg (0.15 mmol) of the Ru-GCN catalyst, 1.06 g (18.8 mmol) of KOH, and 2.0 g (18.8 mmol) of NaH_2PO_2 were charged and 30 mL of the solvent (1:1 mixture of EtOH + H_2O) was added. Then, the autoclave was purged with N_2 gas three times to remove dissolved oxygen at RT. The reaction mixture was heated

to 110 °C on oil bath and maintained at 110 °C for 8 h to obtain complete conversion. After completion of the reaction, catalyst was separated by centrifugation and washed with EtOH. Then, EtOH solvent was completely removed at rotary evaporator. pH of the reaction mixture was adjusted to 7.0 with dilute acetic acid. The product was isolated by extraction with ethyl acetate. Then, the ethyl acetate layer was evaporated on rotary evaporator to receive the crude product. The latter was further purified using a silica gel column with the mixture of ethyl acetate and hexane as diluents to get the pure product (1.05 g, Yield = 92%).

References

- Greene, T.W.; Wuts, P.G. *Protective Groups in Organic Synthesis*; John Wiley & Sons: Hoboken, NJ, USA, 1999.
- Yakukhnov, S.A.; Ananikov, V.P. Catalytic transfer hydrodebenzylation with low palladium loading. *Adv. Synth. Catal.* **2019**, *361*, 4781–4789. [\[CrossRef\]](#)
- Weissman, S.A.; Zewge, D. Recent advances in ether dealkylation. *Tetrahedron* **2005**, *61*, 7833–7863. [\[CrossRef\]](#)
- Wuts, P.G.M. *Greene's Protective Groups in Organic Synthesis*; John Wiley & Sons: Hoboken, NJ, USA, 2014.
- Zhou, L.; Wang, W.; Zuo, L.; Yao, S.; Wang, W.; Duan, W. Selective debenzylation of aromatic benzyl ethers by silica-supported sodium hydrogen sulfate. *Tetrahedron Lett.* **2008**, *49*, 4876. [\[CrossRef\]](#)
- Jensen, R.K.; Thykier, N.; Enevoldsen, M.V.; Lindhardt, A.T. A high mobility reactor unit for r&d continuous flow transfer hydrogenations. *Org. Process Res. Dev.* **2017**, *21*, 370–376.
- Lednicer, D. *The Organic Chemistry of Drug Synthesis*; John Wiley & Sons: Hoboken, NJ, USA, 2007; Volume 8.
- McNair, R. Catalytic deprotection depro catalyst kit/catalytic deprotection. *Aldrich ChemFiles* **2009**, *9*, 21.
- Yin, J.; Weisel, M.; Ji, Y.; Liu, Z.; Liu, J.; Wallace, D.J.; Xu, F.; Sherry, B.D.; Yasuda, N. Improved preparation of a key hydroxylamine intermediate for relebactam: Rate enhancement of benzyl ether hydrogenolysis with dabco. *Org. Process Res. Dev.* **2018**, *22*, 273–277. [\[CrossRef\]](#)
- Oba, M.; Kojima, K.; Endo, M.; Sano, H.; Nishiyama, K. Palladium-catalyzed transfer hydrogenation of organic substrates by hypophosphite in water containing a nonionic surfactant. *Green Chem. Lett. Rev.* **2013**, *6*, 233–236. [\[CrossRef\]](#)
- Mauriello, F.; Ariga-Miwa, H.; Paone, E.; Pietropaolo, R.; Takakusagi, S.; Asakura, K. Transfer hydrogenolysis of aromatic ethers promoted by the bimetallic Pd/Co catalyst. *Catal. Today* **2020**, *357*, 511–517. [\[CrossRef\]](#)
- Pandarus, V.; Béland, F.; Ciriminna, R.; Pagliaro, M. Selective debenzylation of benzyl protected groups with siliacat Pd (0) under mild conditions. *ChemCatChem* **2011**, *3*, 1146–1150. [\[CrossRef\]](#)
- Yamamoto, Y.; Shimizu, E.; Ban, K.; Wada, Y.; Mizusaki, T.; Yoshimura, M.; Takagi, Y.; Sawama, Y.; Sajiki, H. Facile hydrogenative deprotection of n-benzyl groups using a mixed catalyst of palladium and niobic acid-on-carbon. *ACS Omega* **2020**, *5*, 2699–2709. [\[CrossRef\]](#) [\[PubMed\]](#)
- Kim, J.K.; Lee, J.K.; Kang, K.H.; Song, J.C.; Song, I.K. Selective cleavage of C–O bond in benzyl phenyl ether to aromatics over Pd–Fe bimetallic catalyst supported on ordered mesoporous carbon. *Appl. Catal. A Gen.* **2015**, *498*, 142–149. [\[CrossRef\]](#)
- Li, L.; Dong, L.; Li, D.; Guo, Y.; Liu, X.; Wang, Y. Hydrogen-free production of 4-alkylphenols from lignin via self-reforming-driven depolymerization and hydrogenolysis. *ACS Catal.* **2020**, *10*, 15197–15206. [\[CrossRef\]](#)
- Zhang, J.; Ibrahim, M.; Collière, V.; Asakura, H.; Tanaka, T.; Teramura, K.; Philippot, K.; Yan, N. Rh nanoparticles with NiOx surface decoration for selective hydrogenolysis of C–O bond over arene hydrogenation. *J. Mol. Catal. A Chem.* **2016**, *422*, 188–197. [\[CrossRef\]](#)
- Ji, J.; Guo, H.; Li, C.; Qi, Z.; Zhang, B.; Dai, T.; Jiang, M.; Ren, C.; Wang, A.; Zhang, T. Tungsten-based bimetallic catalysts for selective cleavage of lignin C–O bonds. *ChemCatChem* **2018**, *10*, 415–421. [\[CrossRef\]](#)
- Wang, H.; Duan, Y.; Zhang, Q.; Yang, B. Effects of sugars, furans, and their derivatives on hydrodeoxygenation of biorefinery lignin-rich wastes to hydrocarbons. *ChemSusChem* **2018**, *11*, 2562–2568. [\[CrossRef\]](#)
- Gómez-Monedero, B.; Ruiz, M.; Bimbela, F.; Faria, J. Selective hydrogenolysis of α 4, β 4, α 5 C–O bonds of lignin-model compounds and lignin-containing stillage derived from cellulosic bioethanol processing. *Appl. Catal. A Gen.* **2017**, *541*, 60–76. [\[CrossRef\]](#)
- Hartung, W.H.; Simonoff, R. Hydrogenolysis of benzyl groups attached to oxygen, nitrogen, or sulfur. *Org. React.* **2004**, *7*, 263–326.
- Oikawa, Y.; Tanaka, T.; Horita, K.; Yonemitsu, O. Selective hydrogenolysis of the benzyl protecting group for hydroxy function with Raney nickel in the presence of the mpm (4-methoxybenzyl) and dmpm (3, 4-dimethoxybenzyl) protecting groups. *Tetrahedron Lett.* **1984**, *25*, 5397–5400. [\[CrossRef\]](#)
- Perosa, A.; Tundo, P.; Zinovyev, S. Mild catalytic multiphase hydrogenolysis of benzyl ethers. *Green Chem.* **2002**, *4*, 492–494. [\[CrossRef\]](#)
- Lange, S.; Formenti, D.; Lund, H.; Kreyenschulte, C.; Agostini, G.; Bartling, S.; Bachmann, S.; Scalone, M.; Junge, K.; Beller, M. Additive-free nickel-catalyzed debenzylation reactions via hydrogenative C–O and C–N bond cleavage. *ACS Sustain. Chem. Eng.* **2019**, *7*, 17107–17113. [\[CrossRef\]](#)

24. Matsagar, B.M.; Kang, T.-C.; Wang, Z.-Y.; Yoshikawa, T.; Nakasaka, Y.; Masuda, T.; Chuang, L.-C.; Wu, K.C.-W. Efficient liquid-phase hydrogenolysis of a lignin model compound (benzyl phenyl ether) using a ni/carbon catalyst. *React. Chem. Eng.* **2019**, *4*, 618–626. [[CrossRef](#)]
25. Bernt, C.M.; Manesewan, H.; Chui, M.; Boscolo, M.; Ford, P.C. Temperature tuning the catalytic reactivity of cu-doped porous metal oxides with lignin models. *ACS Sustain. Chem. Eng.* **2018**, *6*, 2510–2516. [[CrossRef](#)]
26. Ren, Y.-L.; Tian, M.; Tian, X.-Z.; Wang, Q.; Shang, H.; Wang, J.; Zhang, Z.C. Highly selective reductive cleavage of aromatic carbon–oxygen bonds catalyzed by a cobalt compound. *Catal. Commun.* **2014**, *52*, 36–39. [[CrossRef](#)]
27. Malara, A.; Paone, E.; Bonaccorsi, L.; Mauriello, F.; Macario, A.; Frontera, P. Pd/fe₃o₄ nanofibers for the catalytic conversion of lignin-derived benzyl phenyl ether under transfer hydrogenolysis conditions. *Catalysts* **2020**, *10*, 20. [[CrossRef](#)]
28. Sun, K.-k.; Lu, G.-p.; Zhang, J.-w.; Cai, C. The selective hydrogenolysis of c–o bonds in lignin model compounds by pd–ni bimetallic nanoparticles in ionic liquids. *Dalton Trans.* **2017**, *46*, 11884–11889. [[CrossRef](#)]
29. Qi, L.; Chamas, A.; Jones, Z.R.; Walter, E.D.; Hoyt, D.W.; Washton, N.M.; Scott, S.L. Unraveling the dynamic network in the reactions of an alkyl aryl ether catalyzed by Ni/γ-Al₂O₃ in 2-propanol. *J. Am. Chem. Soc.* **2019**, *141*, 17370–17381. [[CrossRef](#)]
30. Bahuguna, A.; Sasson, Y. Formate-bicarbonate cycle as a vehicle for hydrogen and energy storage. *ChemSusChem* **2021**, *14*, 1258–1283. [[CrossRef](#)]
31. Yang, S.; Jeong, S.; Ban, C.; Kim, H.; Kim, D.H. Catalytic cleavage of ether bond in a lignin model compound over carbon-supported noble metal catalysts in supercritical ethanol. *Catalysts* **2019**, *9*, 158. [[CrossRef](#)]
32. Chakraborty, S.; Bahuguna, A.; Sasson, Y. Advantage of using NaH₂PO₂ over alkali metal formates as a hydrogen source for pd-gc₃n₄ catalyzed hydro-dehalogenation of aryl halides. *ChemistrySelect* **2021**, *6*, 9477–9488. [[CrossRef](#)]
33. Bahuguna, A.; Chakraborty, S.; Sasson, Y. Nio–ni/graphitic carbon nitride as a selective catalyst for transfer hydrogenation of carbonyl compounds using NaH₂PO₂ as a hydrogen source. *Int. J. Hydrogen Energy* **2021**, *46*, 28554–28564. [[CrossRef](#)]
34. Xu, J.; Zhang, L.W.; Shi, R.; Zhu, Y.F. Chemical Exfoliation of Graphitic Carbon Nitride for Efficient Heterogeneous Photocatalysis. *J. Mater. Chem. A* **2013**, *1*, 14766–14772. [[CrossRef](#)]